Appraisal of measurement methods, chemical composition and sources of fine atmospheric particles over six different areas of Northern Belgium

László Bencs[a‡], Khaiwal Ravindra[a,b], Johan de Hoog[a], Zoya Spolnik[a], Nico Bleux[c], Patrick Berghmans[c], Felix Deutsch[c], Edward Roekens[d], René Van Grieken[a]

[a] Micro and Trace Analysis Centre, Department of Chemistry, University of Antwerp, Universiteitsplein 1, B-2610 Antwerp, Belgium
[b] Centre for Atmospheric and Instrumentation Research (CAIR), University of Hertfordshire, Hatfield, AL10 9AB, United Kingdom
[c] Flemish Institute for Technological Research (VITO), Boeretang 200, B-2400 Mol, Belgium
[d] Flemish Environment Agency (VMM), Kronenburgstraat 45, B-2000 Antwerp, Belgium

Abstract –

Daily and seasonal variation in the total elemental, organic carbon (OC) and elemental carbon (EC) content and mass of $PM_{2.5}$ were studied at industrial, urban, suburban and agricultural/rural areas. Continuous (optical Dustscan, standard tapered element oscillating microbalance (TEOM), TEOM with filter dynamics measurement system), semi-continuous (Partisol filter-sampling) and non-continuous (Dekati-impactor sampling and gravimetry) methods of $PM_{2.5}$ mass monitoring were critically evaluated. The average elemental fraction accounted for 2-6 % of the $PM_{2.5}$ mass measured by gravimetry. Metals, like K, Mn, Fe, Cu, Zn and Pb were strongly inter-correlated, also frequently with non-metallic elements (P, S, Cl and/or Br) and EC/OC. A high OC/EC ratio (2-9) was generally observed. The total carbon content of $PM_{2.5}$ ranged between 3-77 % (averages: 12-32 %), peaking near industrial/heavy trafficked sites. Principal component analysis identified heavy oil burning, ferrous/non-ferrous industry and vehicular emissions as the main sources of metal pollution.

Capsule: This work compares $PM_{2.5}$ monitoring methods to characterize $PM_{2.5}$ over six locations of different anthropogenic activities over Northern Belgium.

Keywords: respirable particles, PM_{10}, heavy metals, mineral content, EDXRF analysis, soot, multivariate analysis, non-exhaust emission.

‡ Correspondence author. Permanent address: Research Institute for Solid State Physics and Optics, Hungarian Academy of Sciences, Budapest, Hungary, E-mail address: laszlo.bencs@ua.ac.be, or bencs@szfki.hu; Tel.: +36-1-392-2222/ ext. 1684; Fax: +36-1-392-2223

1. Introduction

The fine fraction of suspended particulate matter (SPM) is generally referred as $PM_{2.5}$ in the literature, i.e., any particle with an aerodynamic diameter below 2.5 μm. Particulates in this size range have been reported to be responsible for adverse health effects in humans (Pope and Dockery, 2006). $PM_{2.5}$ aerosols also affect the local air quality of populated areas by impairing visibility and contribution to acid precipitation (IPCC, 2007; Harrison et al., 2004). Fine particulates play a direct role in global climate change by absorbing and scattering the solar radiation, thereby altering the total radiation budget of the Earth-atmosphere system (IPCC, 2007), and an indirect role by changing the depth and albedo of clouds (Twomey, 1974; IPCC, 2007). Due to the complexity in composition and impacts of $PM_{2.5}$ aerosols, in addition to the need for their physical and chemical characterisation (e.g., metal content), it is also important to determine their sources, how they are formed, their distribution, and local and global transport mechanisms to achieve a better understanding of these aerosols, and to evaluate their risks to human health (Maenhaut, 2008).

Over most of the $PM_{2.5}$ size range, carbonaceous particles in the atmosphere have been shown to be composed of elemental carbon (EC) and organic carbon (OC) (Putaud et al., 2004). The EC has a chemical structure close to that of impure graphite (Chen et al., 2003). EC originates from direct emission of particles from various anthropogenic sources, mainly from combustion (e.g., diesel engines) (Lim et al., 2002). OC originates from both direct emission of particles and atmospheric transformation of organic (gaseous) compounds. Secondary OC has been reported to be generated by condensation of low vapour pressure products during the photooxidation of hydrocarbons (Chow et al., 1996).

In the present study, daily, seasonal and site-specific variations in the elemental, EC and OC content and the mass of $PM_{2.5}$ aerosols were evaluated to identify their chemical composition and sources at six locations of diverse anthropogenic influence in Northern Belgium. Furthermore, continuous, semi-continuous and non-continuous sampling and/or monitoring techniques and analytical chemical methods were applied and critically assessed to aid the decision-making process for $PM_{2.5}$ monitoring and to reduce the bias in the environmental analyses performed.

2. Experimental

2.1. Sampling site characteristics

Six sampling sites, representative of different anthropogenic influences in Northern Belgium (called as Flanders, Fig. 1), were selected: (1) Petroleumkaai (industrial site), the harbour of Antwerp surrounded with several petroleum processing plants, oil refineries and other oil industrial plants; (2) Borgerhout, one of the central districts of Antwerp with high density urban traffic (40-50 thousand cars/day) and also influenced by a non-ferrous industrial site of Hoboken within 5 km distance – a nearby district of Antwerp; (3) Zelzate (suburban site) – at the junction point of a busy main-road of the town with three smaller roads (but lower traffic density than that at Borgerhout) and a petrol station, close to a heavily travelled motorway (A11) and a highway (R4), and also nearby steel industry; (4) Hasselt (suburban site, channel-side with modest traffic density, i.e., shipping at nearby sluice gates and highway with medium/low traffic intensity); (5) Wingene (rural, agricultural area), negligibly low traffic, but certain agricultural activities (animal farming and crops); and (6) Mechelen (outskirts), relatively low traffic density, and some industrial impact, i.e., production of dyes and washing powder. Each location was visited in two, non-concurrent campaigns in diverse seasons of the year (Table 1). The most important meteorological parameters, such as wind-speed (WS), wind direction (WD), relative humidity (RH), air temperature (T_a), air pressure (P_a) and the half hourly amount of precipitation (PR) were also recorded during the sampling campaigns at weather stations located near the sampling sites.

2.2. Sampling of particulate matter

2.2.1. Continuous monitoring

For the continuous monitoring of $PM_{2.5}$, Rupprecht & Patashnick (R&P, Thermo Fischer Scientific, East Greenbush, NY, USA) Model 1400 tapered element oscillating microbalance (TEOM) units were used, each fitted with a $PM_{2.5}$ Sharp-Cut Cyclone inlet. The inlet was preheated to 40 ^{o}C or 50 ^{o}C, to eliminate the effect of condensation or evaporation of water particles. For a short period in Borgerhout, a TEOM was equipped with a filter dynamics measurement system (FDMS), which calculates PM-concentrations based on separate ambient air and reference (at 4 ^{o}C)

measurements. Using a splitter, the sampled air is alternately sent for 6 min to the measurement (at the conditioning temperature of 30-50 ^{o}C), either directly, or after filtration at 4 ^{o}C. Thus it can be used to detect the vaporization losses encountered with a standard TEOM. The concentration of $PM_{2.5}$ was also optically monitored (i.e., scattering measurements) with the application of an R&P Dust Monitor (Dustscan).

2.2.2. Non-continuous sampling and gravimetry

Daily (24 h), size-fractionated aerosols at a height of ~1.8 m above ground level were occasionally sampled using a four-stage Dekati-impactor with an airflow rate of 30 dm^3 min^{-1}. Nuclepore-filters with a diameter of 25 mm and a pore-size of 0.2 μm were fitted onto the three, upper-stage impactor-plates, corresponding to >PM_{10}, $PM_{10-2.5}$, and $PM_{2.5-1,}$ fractions, respectively. A Whatman filter with a diameter of 47 mm was placed onto the bottom of the impactor to collect the "back-up" (PM_1) fraction. The filters were weighed on a micro-balance (Sartorius model M5P-000V001, Göttingen, Germany) before and after sampling according to the EN12341 protocol. The TSP, PM_{10}, and $PM_{2.5}$ data were calculated from the masses of diverse fractions deposited on the different stages of the impactor.

2.2.3. Daily sampling of $PM_{2.5}$ and PM_{10} for EDXRF analysis

Automated R&P Model Partisol Plus samplers and an ESM Eberline Model FH95 SEQ (Eberline Instruments GmbH, Germany) were used for the daily sampling of $PM_{2.5}$ and PM_{10}, respectively, with an airflow rate of 1 m^3 h^{-1}. Various types of filters of 47 mm diameter and 0.8 μm porosity were tested, e.g., Teflon, cellulose nitrate, and cellulose acetate. The latter filter material was used for sampling the total elemental content, since it gave the lowest blanks for XRF-analysis. After removing the samples from the sampling instruments, they were stored in a cooling box and transported to the laboratory, where they were kept in a fridge (below 4^{o}C) till sample processing. The filters were subjected to gravimetric analysis (see Section 2.2.2.). However, the gravimetric analysis of the cellulose acetate filters was influenced by the tendency to be electrostatically charged,

which resulted in a certain deviation in the measured filter masses. For this reason, only the gravimetric results for Teflon-filters were taken into consideration.

2.3. Analytical methods and instrumentation

2.3.1. Energy dispersive X-ray fluorescence spectrometry (EDXRF)

The EDXRF analysis was performed on a Tracor Spectrace 5000 instrument, which uses a low power Rh-anode X-ray tube (17.5 W). The characteristic X-ray radiation was detected by a Si(Li) detector. For determining high-Z elements (starting from K), an accelerating voltage of 35 kV and a current of 0.35 mA were used. The acquisition time was set at 10000 s. Low-Z elements (from Al to Cl) were measured at 10 kV and 0.35 mA with an acquisition time of 4000 s. The measured intensities were converted into elemental concentrations by the AXIL (analysis of X-ray spectra by non-linear iterative least-squares) program (Vekemans et al., 1994). The limit of detection (LOD) values for Al, Si, K, Ca, Ti, V, Cr, Mn, Fe, Ni, Cu, Zn, Se, Br, Rb, Sr and Pb ranged from 3.8 to 12.6 ng m^{-3} for air samples. The precision of the determinations expressed as the relative standard deviation (RSD) was generally better than 1 % for the high-Z elements, but it was around 5 % for Al, Si, P, S and Cl (Samek et al., 2002).

2.3.2. Monitoring of organic and elemental carbon

Particulate carbon was monitored with an Ambient Carbon Particulate Monitor (ACPM) Model 5400 (R&P) fitted with a Stairmand $PM_{2.5}$ cyclone head. Air was sampled at a flow-rate of 16.7 l min^{-1} on the impaction plate (with a 50 % effective aerosol cut-off diameter of 0.14 µm) of the ACPM preheated at 50 °C to avoid the adsorption of gaseous organic compounds. The sampling interval was set at 2 h. As a first stage of the analysis, the samples were heated up to 340 °C to decompose the organic species deposited. This step was followed by afterburning at 750 °C. After each analysis step, performed in a closed loop under atmospheric air, the CO_2 concentration was measured with a non-dispersive infrared detector, and the carbon content was calculated. The concentrations obtained after the first and the second analysis stage correspond to the fractions of OC and EC, respectively.

It is to be noted that the ACPM may suffer from positive sampling artifacts, which depend on the working-temperatures of its impactor plate (Matsumoto et al., 2003). However, the influence of these artifacts on the measurement of OC collected for longer sampling intervals (e.g., 2 h), especially at its higher concentrations, and evolved at a higher temperature (250-340 ^{o}C) and EC in aerosols could involve less uncertainty (Matsumoto et al., 2003). It should also be mentioned that EC readings from the standard ACPM have been found to be lower than those from a modified-ACPM, due to the fine aerosol cut-off, as above (ten Brink et al., 2005). Because of this negative bias, the standard ACPM technique is just reliable in a sense to make an estimation of the EC/OC values.

2.4. Data evaluation and statistics

The analytical data were statistically treated using the SPSS software package (version 14.0). Bivariate correlation analysis was performed by calculating the Pearson's correlation coefficient at two-tailed significance levels (i.e., corresponding to correlations significant either at the p=0.05 or p=0.01 levels, respectively). The daily metal levels were also processed using the principal component analysis (PCA) with varimax rotation and Kaiser Normalization. Only principal components (PCs) having an eigenvalue in the component data set higher than unity before varimax rotation were retained.

3. Results and discussion

3.1. Assessment of $PM_{2.5}$ dust monitoring methods

3.1.1. Bias experienced with optical methods

The temporal evolution of the $PM_{2.5}$ mass curves from the optical Dustscan was very similar to those of gravimetric methods, but its absolute values were strikingly higher (Fig. 2). Since this mass deviation rather randomly changed, it was not possible to specify an exact factor/function for this inaccuracy. Dustscan, like other optical methods, is usually calibrated against so-called "standard aerosols". However, the morphology and composition of atmospheric aerosols can change rapidly over time and location, which can cause a bias in the optical measurements.

3.1.2. TEOM versus gravimetric particulate measurements

The $PM_{2.5}$ levels from gravimetry were significantly higher than those of the standard TEOM (Fig. 3). This bias is due to the temperature conditioning of the air stream in the TEOM (cf. Section 2.2.1.), which treatment can cause mass loss through evaporation of volatile components in $PM_{2.5}$, e.g., ammonium nitrate (NH_4NO_3) (Charron et al., 2004), semi-volatile organic compounds (Vecchi et al., 2009), and water attached to aerosol particles due to their hygroscopic nature, even at as low temperatures as 25-30 ^oC. This finding was verified by simultaneous monitoring of $PM_{2.5}$ in Mechelen in the second campaign with two TEOM units, applying conditioning temperatures of 50 ^oC and 40 ^oC, respectively (Table 2). A Partisol sampler working at 20 ^oC was used as a reference. No mathematical correction for NH_4NO_3 evaporation losses was applied in these experiments, as usually recommended when applying standard TEOM methods (Charron et al., 2004). It is to be noted that NH_4NO_3 has been found in $PM_{2.5}$ in concurrent samples of the same sites (Bencs et al., 2008). As expected, an increase in the conditioning/sampling temperature resulted in a decrease in the daily $PM_{2.5}$ mass (see Table 2 and Fig. 3).

Comparing the standard TEOM and TEOM-FDMS results, an obvious discrepancy can be seen between the two $PM_{2.5}$ data series (Fig. 3). On the other hand, the TEOM-FDMS values approach very well those from Partisol sampling and gravimetry. Thus they exhibit a more accurate monitoring of $PM_{2.5}$ than the methods involving the use of mathematical correction factors.

Interestingly, the $PM_{2.5}$ mass data in Mechelen showed a contradicting trend (Fig. 4), i.e., a reverse pattern on most sampling days (i.e., Partisol< TEOM (40 ^oC) < TEOM (50 ^oC)). The same trend could be observed for Petroleumkaai in the 1st campaign and for Wingene and Zelzate in the 2nd campaign. Moreover, the PM_{10} results of TEOM and Eberline appeared to behave the same way. The change in the daily average temperature (T_{da}) may offer a possible explanation. On those days, when the expected difference between $PM_{2.5}$ data of TEOM and gravimetry did not occur, T_{da} was always higher than 15 ^oC, which led to the following conclusions:

(1) When the ambient air temperature is high enough (e.g., T_{da} > 15 °C), a part of the volatile compounds is already evaporated before/during sampling. Therefore, the temperature conditioning in TEOM has a less pronounced, or even negligible effect on $PM_{2.5}$ values, i.e., the data are in

agreement independently of the temperature of conditioning. Since the Partisol filters were measured passing some days (sometimes two weeks) after the sampling, they were longer exposed to fluctuating outdoor conditions and generally higher indoor (laboratory) temperatures than the outdoor temperatures. This can cause additional evaporation of volatile sample components, which results in $PM_{2.5}$ values lower than those obtained from TEOM.

(2) When T_{da} is lower than 15 °C, the conditioning effect in TEOM is larger and the Partisol filters are preserved much better during their stay in the sampling units, due to the low evaporation losses.

(3) The fact that PM_{10} concentrations are less dependent on T_{da} during summer campaigns, could be explained by the fact that relatively coarser particles are present in the air and a considerable part of NH_4NO_3 exists in air by evaporation, due to the drier and warmer weather. Certainly, the coarse particles present in the $PM_{10-2.5}$ fraction are less prone to vaporization than most fine particles in $PM_{2.5}$. The fine particles can be more easily vaporized than coarse particulates, due to the changing in their solid state characteristics with a decreasing aerodynamic diameter (e.g., melting and boiling point). That's why, their masses affect the PM_{10} measurements to a larger extent, and the influence of T_{da} does not prevail so clearly. In cold periods with a high precipitation rate, such as in Mechelen in the second campaign (Table 1), the less coarse particles remain in the air. Hence, PM_{10} could evidently be more influenced by evaporation effects.

3.1.3. Site-specific variation in the levels of $PM_{2.5}$

The highest average daily concentrations of $PM_{2.5}$ were observed in Borgerhout, i.e., 29±15 µg m^{-3} and 45±22 µg m^{-3} for the first and second campaigns, respectively (Table 3). The highest daily mean concentration of $PM_{2.5}$ was also experienced in Borgerhout (99.7 µg m^{-3}) in the second campaign. A strong linear correlation was found between the $PM_{2.5}$ and PM_{10} concentrations. The $PM_{2.5}$ contribution to the PM_{10} levels was the highest in Borgerhout (i.e., 71% on average; and 92% maximum), which means that most of the particles were present in the fine to ultra-fine particle range at this site.

In view of the new European Directive (ED), it might be interesting to evaluate the measured concentrations and to check if they meet the proposed $PM_{2.5}$ limit values of yearly average of 25 μg m^{-3} (European Directive, 2008). Since only a maximum of three-month-long monitoring was carried out at each location, it was only possible to make a prediction based on extrapolation with this limited data set. These daily average $PM_{2.5}$ values have already exceeded the ED-limit for three sites in the first campaign and for Borgerhout in the second campaign (Table 3). However, if taking into account the overall campaign averages, only the levels at Borgerhout (38 μg m^{-3}) were found above the ED-limit (Table 4).

The average yearly concentration of $PM_{2.5}$ at each sampling location was calculated by an extrapolation scheme using the average daily $PM_{2.5}$ concentrations for the sampling campaigns at each site and a correction factor based on the proportion of the average concentrations monitored during the same period and over a whole year at other three reference locations. In this way, it was possible to avoid over- or underestimations, due to unforeseen, general seasonal variations. The yearly average $PM_{2.5}$ concentration for the three reference locations (Mechelen-Zuid, Mechelen-Nekkerspoel and the Brussels-Zaventem) in 2002 was 16 μg m^{-3}; the average for the same period as in Borgerhout was 21 μg m^{-3} (Table 4). These results are also in agreement with the annual mean $PM_{2.5}$ level of 17 μg m^{-3} reported for Menen, Belgium (Ravindra et al., 2008). Therefore, one could already assume that the very high average value of 38 μg m^{-3} in Borgerhout was due to measurements that were carried out in an episodic pollution period with very high $PM_{2.5}$ levels. Thus the yearly average for Borgerhout is expected to be lower than 38 μg m^{-3}. According to the results of extrapolation (Table 4), only the Borgerhout site would not meet the ED-limit.

3.1.4. Impact of meteorological conditions on the $PM_{2.5}$ and PM_{10} mass

As would be expected, an increase in wind speed, precipitation, and/or RH decreased the $PM_{2.5}$ and PM_{10} levels (Supplementary Table 1). On the other hand, an increase in the air temperature would be generally followed by an increase in the aerosol mass, i.e., particle accumulation. However, this trend was experienced only for a couple of sites, like Borgerhout during the winter-spring and Wingene in the summer campaign, while T_a was rather anti-correlated with both $PM_{2.5}$

and PM_{10} aerosols at the other sites/campaigns. This was likely due to the fairly high percent of volatile fraction of aerosols, e.g., NH_4NO_3 (Bencs et al., 2008), the increase in T_a allowed their vaporization in both particulate fractions.

3.2. Elemental composition of $PM_{2.5}$

3.2.1. Ratio of elements in $PM_{2.5}$

The elemental content was found to be at a relatively low, but highly fluctuating percentage in $PM_{2.5}$, ranging from 0.1 to 24 % with an average of 3.4 % (Table 5). As a general observation, peak levels of elements in $PM_{2.5}$ (i.e., values generally higher than 10 % of the total $PM_{2.5}$ mass) were found at sites with industrial impact (Zelzate, Mechelen and Petroleumkaai). In Hasselt, the elemental fraction was higher only in the second campaign, which is likely due to some industrial impact as well as the ship-traffic nearby this location, and the prevailing winds from the west. As expected, at the rural site of Wingene a lower percentage of elements were found in $PM_{2.5}$, i.e., up to 6.3 %, when the maximum observations were considered. These findings show the importance of industrial emission of metals and the lower impact of the traffic. The calculated total-element-to-$PM_{2.5}$ ratios are comparable with those observed for the city of Ghent in Belgium (3-4 %) (Viana et al., 2007) and for Central European cities (2-5 %), but much lower than those for North and South European cities with values of 15-40 % and 8-20 %, respectively (Querol et al., 2004).

3.2.2. Influence of anthropogenic activities on the elemental content of $PM_{2.5}$

The elemental content in $PM_{2.5}$ showed high site-specific variations (Table 6). Non-metallic elements, such as P, S, Cl, Se and Br, were also detected at significant air levels, ranging from 14-302, 9.9-4600, 9-2400, 1.1-28 and 2-91 ng m^{-3}, respectively. The highest total concentrations of elements were found at sites under industrial influence (Zelzate, Petroleumkaai, and Borgerhout). The cold seasons were characterized with increased metal content of $PM_{2.5}$ (e.g., K, V, Fe, Ni, and Zn). The total elemental content (200-1100 ng m^{-3}), irrespective of the nature of the sampling site, is commensurate with those data reported for Central European cities (Vallius et al., 2005) and for

Ghent (Viana et al., 2007), but generally lower than those from North and South European cities with 1000-6000 ng m^{-3}, respectively (Querol et al., 2004).

Fairly high concentrations of Al, Si, K, Ca and Fe, i.e., up to a few hundred ng m^{-3}, were generally found at each site (Table 6). Most of these elements have a crustal origin (Maenhaut et al., 2007), although some of them in $PM_{2.5}$ may have an anthropogenic origin. For instance, Oravisjärvi et al. (2003) have pointed out Li, F, Na, Mg, Al, K, Ca, Mn, Fe, Zn, Cd and Pb at enhanced atmospheric levels in the vicinity of steel-works. Most of these elements were also found at increased air levels at Zelzate (Table 6). At this area, F has also been observed at a bit enhanced level compared to the other sites (Bencs et al., 2008). The highest K content was found at Borgerhout during the cold season, which is likely due to the presence of biogenic materials (e.g., wood and coal combustion). Similarly high K levels were observed in Zelzate during winter and also in Hasselt during autumn.

Zn and Pb were present at lower levels than the former elements, but still at significant concentrations (Table 6). The highest levels were at industrial/heavy trafficked sites (Zelzate and Borgerhout). Pb is also associated with non-biomass burning sources, like fossil fuel combustion and the non-ferrous industry (Nriagu and Pacyna, 1988). The nearby presence of a precious metal refinery in Hoboken, i.e., within 5 km of the sampling site of Borgerhout, supports this possibility. Also, coal-burning (e.g., in power stations) can be an emission source of Zn and Pb, as well as increase the air concentrations of other heavy metals like Cr, Ni, Cu and Cd (Keegan et al., 2006). In urban areas, the brake lining of vehicles is a major source of Cu, Zn, Cd, Sb and Pb (Hjortenkrans et al., 2007).

Ti, V, Cr, Mn, Ni, Cu and Rb were present at levels lower than ~10 ng m^{-3} in $PM_{2.5}$ (Table 6). Sr was measured in well detectable amounts only at Zelzate during the first campaign (average: 1 ng m^{-3}), which is likely due to the nearby steel industry. Cu was found at elevated levels at the heavy trafficked Borgerhout. V and Ti were detected at increased atmospheric concentrations at the industrial/heavy trafficked sites. Interestingly, V was also observed at fairly enhanced levels at the agricultural Wingene during both campaigns. This could be due to the heavy diesel emission from

vehicles used over the crops. The V-to-Ni ratio of ~2 supports this assumption (Maenhaut et al., 2007).

3.3. Source identification of elements in $PM_{2.5}$

3.3.1. Correlation analysis

3.3.1.1. General trends over sites and campaigns

Some of the elements, mostly originating from anthropogenic emissions, like K, Mn, Fe, Cu, Zn and Pb, further referred to as the "base-group", were strongly correlated with each other (Supplementary Table 1). Moreover, they were frequently correlated with non-metallic elements, like P, S, Cl and/or Br, and also with EC and OC. The correlation of Fe, Zn, Cu, Ba and EC suggests traffic/vehicular sources (Viana et al., 2008).

Generally, the anthropogenic elements were strongly correlated with elements mostly of crustal origin, e.g., Al, Ca, and/or Si, Ti. Monitoring data from a background site indicate Si-Al-Fe-, Si-, Ca-S-Si-, Ca-Si-, Fe-Si-, and Ti-Si-rich particles as typical soil elements (Hoornaert et al., 2004). These elements in $PM_{2.5}$ can also originate from anthropogenic sources. However, an enrichment factor of higher than unity has been observed only for Ca and Ti over Uccle, an urban background site in Belgium, i.e., 10 and 3, respectively (Maenhaut et al., 2007). Therefore, a rather crustal origin has been presumed for the atmosphere over Flanders.

Cr was usually correlated with some elements of the base-group, which points to common sources. Cr is mostly associated with traffic/vehicular emission (Viana et al., 2008; Hu et al., 2009) and industrial combustion (e.g., coal-fuelled power plants (Keegan et al., 2006) and coke ovens (Wang et al., 2003)). Ni was correlated with Cu over most of the sites, which can be interpreted as a signature of oil combustion (Pio et al., 1989). Rb was generally well correlated with EC, OC and the elements of the base-group at sites with industrial influence. Sr was usually correlated with Al and/or Si, which shows its origin mostly of crustal sources. The most interesting site/campaign-specific correlations are discussed as follows.

3.3.1.2. Site- and campaign-specific correlations

In Zelzate, besides the base-group, K was also correlated with Ni and Sr, in the winter campaign, and with V and Rb in the summer-autumn campaign. These elements and Fe were closely correlated to each other in both campaigns, thus they most probably originate from the neighbouring steel industry. Interestingly, they were also correlated with Al and/or Si, which is usually of crustal origin, but for Al studies also suggest combustion related sources in $PM_{2.5}$ (e.g., steel industry – Oravisjärvi et al., 2003). In the winter campaign, Ca was correlated well with P, Ni and Cu, which suggests that a part of the Ca likely comes from re-suspended road dust. In the winter campaign, V was well correlated with Br and P, but in the summer-autumn campaign, it was strongly correlated with Ni and Si. According to Maenhaut et al. (2007), V and Ni have a source of vehicular emission and heavy oil burning. At Zelzate, V likely originates from the diesel traffic, but also, a part of it might come from the re-suspended road dust, as observed by Oravisjärvi et al. (2003). Ti might originate partly from the steel industry, since it was strongly correlated with Fe and the other steel-industry related elements as above and EC in the summer-autumn campaign, but a part of it might also come from crustal sources (Maenhaut et al., 2007) and/or re-suspended road dust (Oravisjärvi et al., 2003).

The emission of a petrochemical plant has been characterized with increased S, V, Ni, Zn and Se content of $PM_{2.5}$ (Bosco et al., 2005), which results in correlation of these elements. In Petroleumkaai, the base-group, EC and OC were correlated with V and/or Ni, which points to a source of the nearby heavy oil burning activities. In the autumn campaign, Ti was correlated with the crustal Al, Si, but also with P and Se, while in the winter campaign, it was strongly correlated with V and Si, thus it partly originates from the oil refinery emissions.

In the heavy trafficked Borgerhout, besides the base-group and crustal elements, Ca was also correlated strongly with Ti, Cr, non-metallic elements and EC, thus they possibly come from road dust re-suspension. Ti was correlated with V, Ni and P in the autumn-winter campaign, while it was correlated with V, Cr, the base-group and crustal elements in the winter-spring campaign. Ni was correlated well with EC and OC in the winter-spring campaign. Thus Ti and Ni were supposed to originate from diesel emissions and heavy oil burning activities, e.g., the oil industry at Petroleumkaai located northwest of Borgerhout.

The suburban/riverside site at Hasselt showed a pattern of strong correlations of the base-group with crustal (Al, Si and Ca) and non-metallic (P, S and Br) elements in both campaigns. Interestingly, Cl was strongly correlated with these elements too. Cl is of sea salt origin (Hoornaert et al., 2003). However, at Hasselt, the origin of Cl might be found in the nearby paper industry, which is a source of organic Cl. Interestingly, Ni was strongly correlated with most of the detected elements, while Ti, V and Cr were somewhat poorly correlated with any of them. V has also been observed to be poorly correlated in $PM_{2.5}$ in Uccle, for which additional sources of Ni (e.g., non-ferrous industry) were presumed to be responsible (Maenhaut et al., 2007). This is likely true for the Mechelen site.

The suburban Mechelen site showed a similar pattern of correlations of elements like that of Hasselt, apart from the non-metallic elements, which were much less correlated with the others. For example, Cl was correlated only with Ca and Ti, thus they likely originated from road dust re-suspension. In the autumn-winter campaign, EC was correlated with Fe, Zn and Pb, .

In the rural/agricultural area of Wingene, the strong correlation of P, S, V, Ni and Br is likely related to the use of diesel vehicles over nearby crops in the spring and summer seasons. In the spring campaign, Ti was correlated with Ni and Br. Thus Ti likely also related to diesel fuel emissions. The correlation of K, Cr, Mn, Fe, Zn, Pb and EC points to biomass burning (cf. Godoi et al., 2004).

3.3.2. Principal component analysis (PCA)

As the PCs were extracted successively, the first PC is more correlated with the variables than the second (Supplementary Tables 2-7). Hence, only the major PCs from each site were assessed for source characterization. The species having loadings above 0.7 were characterized "high" and those below 0.4 "low". The species having PC loading of less than 0.4 were considered either not be related to the other species or were explored in an additional PC (Costello and Osborne, 2005).

PC 1 for Petroleumkaai shows high loadings for P, S, K, Fe, Cu, Zn, and Pb. This PC indicates the presence of petroleum refinery and other industrial combustion activities, which are dominant in this area. Further, PC 2 has high loadings of Al and Si with moderate loadings of Ca and Rb. This PC reflects the contribution of crustal elements. At Borgerhout, PC 1 is highlighted by Al, Si, P, S and K with moderate loadings of Cl, Ca, V, Fe, Zn, Br and Pb. This PC shows a mixed

influence of vehicular emission and suspension of road dust. Zn has been identified in tire wear emission and Fe in brake-drum abrasion (Manoli et al., 2002). PC 2 has high Fe and Cu loadings with relatively lower loadings of Ca, Zn, Sr and Pb. This PC is indicative of non-exhaust emission sources (e.g., wheel/brake abrasion of vehicles) with the influence of diesel exhaust, as well as the influence of a nearby precious metal refinery. Although Pb has been phased out from petrol, generally, road traffic emission remains one of the sources (Heal et al., 2005). Zelzate has high loadings of Al, Cl, K, Zn, Br and Pb, Fe, with moderate loadings of Si, P, S, and Cu. This emission seems to be related to the coke-oven industries in this area. PC 2 is represented by P, S and Cr suggestive of the combustion activities in the vicinity.

PC 1 in Hasselt has high loadings of Si, S, Cl, K, Ca, Ni, Cu, Zn, Br and Pb, which shows the mixed influence of natural and vehicular/ship emissions. PC 2 is represented by Cr and Fe. High loadings of Fe and Cr are suggestive of road dust (Manoli et al., 2002), but considerable Cr comes also from mobile sources (e.g., brake wear emissions) nearby heavily trafficked roads (Hu et al., 2009). At Wingene, K, Fe, Zn and Pb show relatively higher PC loadings. In addition to the crustal sources, K has been identified an important marker of biomass burning. Wingene is characterised as a rural/agricultural area, thus biomass burning activities may be expected in this area. PC 2 has high loadings of V, Mn and Ni. V and Ni are markers of fuel-oil (Heal et al., 2005), whereas the other elements are likely due to local suspension of dust during agricultural practices. PC 1 at Mechelen is highlighted by Al, Cl, K, Ca, Cu, Zn, Se and Br. Interestingly, high loadings of Br and Se were noticed only at this location. Br is frequently used in dye industries; whereas Se is mainly used in glass manufacturing chemicals and pigments. This PC shows the influence of local industrial activities on $PM_{2.5}$ composition. PC 2 has high loadings of Si, P, S, Fe, Rb and Pb. Some of these elements can be related to the re-suspension of road dust (Heal et al., 2005), and hence, indicate their relation with non-exhaust emissions. However, the presence of S and P also indicates industrial combustion and biomass burning activities, respectively.

3.4. Elemental carbon and organic carbon content of $PM_{2.5}$

3.4.1. Site-specific variation of EC and OC

The daily concentrations of EC and OC determined non-concurrently with the ACPM over various sites/campaigns are listed in Table 7. The minimum levels of EC ranged between 0.1-0.5 μg m^{-3}, while the maximum EC values were found to be between 1.1-4.4 μg m^{-3}. Amongst the studied sites, Borgerhout and Petroleumkaai reported the highest EC levels in the first campaign, with values of 3.3 and 4.4 μg m^{-3}, respectively. The average level of EC was the highest also at the heavy trafficked Borgerhout (1.3-1.5 μg m^{-3}), whereas sites with less traffic density showed much lower concentrations (0.3-0.6 μg m^{-3}). The exception was Petroleumkaai, with an increased average value of 1.1 μg m^{-3} in the first campaign, likely due to the nearby industrial emissions combined with warmer weather conditions. The maximum daily OC values were found to be at Mechelen (10 μg m^{-3}) and Petroleumkaai (7.3-7.6 μg m^{-3}), and followed a similar pattern for the average levels of 4.1 and 4.2 μg m^{-3}, respectively.

In the literature, OC is often expressed as organic material (OM). To calculate OM, multiplication factors of 1.6 and 2.1 for OC have been recommended for urban and non-urban aerosols, respectively (Turpin and Lim, 2001). In this study, the factor of 1.6 was used for calculating the OM values (Table 7). Fairly low average levels of EC and OC were observed for each site/campaign, i.e., ranging between 0.4-1.5 and 2.3-4.2 μg m^{-3}, respectively (Table 7), which correspond to an OM+EC range of 4.1-7.7 μg m^{-3}. This interval is similar to those OM+EC values, reported for the total carbon content of $PM_{2.5}$ in Ghent, Belgium (3.9-9.7 μg m^{-3}) (Viana et al., 2007) and to those OC+EC ranges for North European cities (1-6 μg m^{-3}) (Querol et al., 2004), but a bit lower than those reported for Central European cities (3-16 μg m^{-3}) (Querol et al., 2004; Putaud et al., 2004).

The two-hour peak values of EC and OC of 19 and 20 μg m^{-3}, respectively, were found at Borgerhout (Table 8). A similar high OC value was found at Petroleumkaai in the first campaign; whereas the EC value was lower (7.4 μg m^{-3}). The highest two-hourly minimum value of EC was observed in Borgerhout (0.44 μg m^{-3}) in winter-spring, whereas the other sites yielded 1-2 orders of magnitude lower values. Interestingly, the highest minimum OC values occurred in Mechelen (1.1 μg m^{-3}) and Hasselt (0.86 μg m^{-3}), which are suburban areas (both influenced by industrial activities),

448 though the less intense, but continuous local emissions by car and ship traffic may contribute to these
449 increased background OC levels.
450
451 3.4.2. OC/EC ratios
452 The primary OC/EC ratio is defined as the atmospheric concentration of organic material
453 emitted directly into the air by anthropogenic sources and measured as primary OC divided by the
454 atmospheric level of EC. In early studies, a primary OC/EC value of 2.2 is assumed to indicate rising
455 secondary organic aerosol (SOA) levels in the atmosphere (Turpin and Huntzicker, 1991). An
456 OC/EC ratio of 2 has also been used to identify the formation of SOAs (Chow et al., 1996). A recent
457 study by Harrison and Yin (2008) suggests a minimum OC/EC ratio of 0.65.
458 For most of the sampling sites, a high OC/EC ratio (3.7-9) was generally observed (Table 7).
459 The exception was the heavy trafficked urban site of Borgerhout with a value of 1.9 in each
460 campaign. Especially high OC/EC ratios of 8.4 and 9 were observed at Mechelen and Hasselt,
461 respectively, the sites with medium-to-low traffic density and some industrial influence. The
462 experienced high OC/EC ratios indicate an intensive formation of SOAs or the contribution of local
463 sources to increase OC levels (e.g., wood burning).
464
465 3.4.3. Contribution of total carbon (EC+OC) to $PM_{2.5}$ levels
466 The minimum levels of total carbon (TC) in $PM_{2.5}$ ranged between 3 and 11 %, while its
467 maximum values were found to be between 22 and 77 % (Table 9). The average contribution of TC
468 was relatively high for Petroleumkaai (32 %), Hasselt (23%) and Mechelen (24 %), whereas the
469 remaining sites were usually below 14 %. Apart from the industrial site of Petroleumkaai, these
470 values are generally lower than those reported for the OM+EC content of $PM_{2.5}$ for Ghent (32-39 %)
471 (Viana et al., 2007), as well as those reported for other European cities (20-45 %) (Viana et al., 2007;
472 Putaud et al., 2004; Querol et al., 2004).
473

4. Conclusions

The results obtained with the assistance of diverse physical and chemical characterisation methods for $PM_{2.5}$ generally showed very similar temporal and spatial changes in the pattern of the studied aerosol components. The optical dust monitoring methods (e.g., Dustscan) produce higher $PM_{2.5}$ mass readings than the gravimetric methods, consequently, they can only be used for showing concentration trends. The $PM_{2.5}$ data from the standard TEOM monitoring are handicapped by sampling artifacts (e.g., evaporation losses), whereas values from the TEOM-FDMS method agreed well with the data from gravimetry. The monitoring over Flanders produced similar results for the $PM_{2.5}$ mass as for other European sites. However, a fairly large difference was found for the elemental and total carbon (OC+EC) contributions in Flanders compared to higher percentages observed in most of the Central European cities. This bias might be due to the use of a standard ACPM in the present experiments, which is handicapped by lower EC/OC readings.

The metal content of $PM_{2.5}$ indicated the high importance of industry-related emissions over Flanders and a lower impact of the traffic emission. PCA and correlation analysis showed the contribution of local traffic, heavy oil burning, combustion, and ferrous/non-ferrous industrial emission, as the main sources to $PM_{2.5}$ levels. It is to be noted that only one of the sampling sites (Borgerhout with heavy traffic and some industrial influence) did not meet the EC's proposed annual limit for $PM_{2.5}$. This is an indicative of "hot-spots" existing in the urban environment, which should be locally monitored for $PM_{2.5}$ levels. Moreover, local legislations on the air quality assurance of these areas should be introduced for counteracting the pollution periods when the dust content is expectable to overtake the daily allowable EC-limit, for example, by immediate actions of local authorities (e.g., by reducing the density of the local traffic).

Acknowledgement

This study presents part of the results obtained in the project "Metingen van $PM_{2.5}$ in Vlaanderen (2001-2003)", for which financial support by the Flemish Environment Agency (Vlaamse Milieumaatschappij) is gratefully acknowledged. One of the authors (L. Bencs) expresses his gratitude for the support by the Hungarian Scientific Research Fund (OTKA) under the project of

502 F67647.

503 **References**

504 Bosco, M.L., Varrica, D., Dongarra, G., 2005. Case study: inorganic pollutants associated with
505 particulate matter from an area near a petrochemical plant. Environmental Research, 99, 18-30.
506
507 Bencs, L., Ravindra, K., de Hoog, J., Rasoazanany, E.O., Deutsch, F., Bleux, N., Berghmans, P.,
508 Roekens, E., Krata, A., Van Grieken, R., 2008. Mass and ionic composition of atmospheric fine
509 particles over Belgium and their relation with gaseous air pollutants. Journal of Environmental
510 Monitoring, 10, 1148-1157.
511
512 Charron, A., Harrison, R.M., Moorsroft, S., Booker, J., 2004. Quantitative interpretation of
513 divergence between PM_{10} and $PM_{2.5}$ mass measurement by TEOM and gravimetric (Partisol)
514 instruments. Atmospheric Environment, 38, 415-423.
515
516 Chen, S.J., Hsieh, L.T., Tsai, C.C., Fang, G.C., 2003. Characterization of atmospheric PM_{10} and
517 related chemical species in southern Taiwan during the episode days, Chemosphere, 53, 29-41.
518
519 Chow, J.C., Watson, J.G., Lu, Z.Q., Lowenthal, D.H., Frazier, C.A., Solomon, P.A., Thuillier, R.H.,
520 Magliano, K., 1996. Descriptive analysis of $PM_{2.5}$ and PM_{10} at regionaly representative locations
521 during SJVAQS/AUSPEX. Atmospheric Environment, 30, 2079-2112.
522
523 Costello, A.B., Osborne, J.W., 2005. Best practices in exploratory factor analysis: four
524 recommendations for getting the most from your analysis. Practical Assessment Research &
525 Evaluation, 10, 1-9.
526
527 European Directive, 2008. Directive 2008/50/EC of the European Parliament and of the Council of
528 21 May 2008 on ambient air quality and cleaner air for Europe. Official Journal of the European
529 Union, L152, 1-44.
530
531 Godoi, R.H.M., Godoi, A.F.L., Worobiec, A., Andrade, S.J., de Hoog, J., Santiago-Silva, M.R., Van
532 Grieken, R., 2004. Characterisation of sugar cane combustion particles in the Araraquara region,
533 Southeast Brazil. Microchimica Acta, 145, 53-56.
534
535 Harrison, R.M., Yin, J., 2008. Sources and processes affecting carbonaceous aerosol in central
536 England. Atmospheric Environment, 42, 1413-1423.
537
538 Harrison, R.M., Jones, A.M., Lawrence, R.G., 2004. Major component composition of PM_{10} and
539 $PM_{2.5}$ from roadside and urban background sites. Atmospheric Environment, 38, 4531-4538.
540
541 Hjortenkrans, D.S.T., Bergbäck, B.G., Häggerud, A.V., 2007. Metal emissions from brake linings
542 and tires: Case studies of Stocholm, Sweden 1995/1998 and 2005. Environmental Science and
543 Technology, 41, 5225-5230.
544
545 Hoornaert, S., Godoi, R.H.M., Van Grieken, R., 2003. Single particle characterization of the aerosol
546 in the marine boundary layer and free troposhphere over Tenerife, NE Atlantic, during ACE-2.
547 Journal of Atmospheric Chemistry, 46, 271-293.
548
549 Hoornaert, S., Godoi, R.H.M., Van Grieken, R., 2004. Elemental and single particle aerosol
550 characterization at a background station in Kazakhstan. Journal of Atmospheric Chemistry, 48, 301-
551 315.
552
553 Heal, M.R., Hibbs, L.R., Agius, R.M., Beverland, I.J., 2005. Total and water-soluble trace metal
554 content of urban background PM_{10}, $PM_{2.5}$ and black smoke in Edinburgh, UK. Atmospheric
555 Environment, 39, 1417-1430.
556
557 Hu, S.-H., Herner, J.D., Shafer, M., Robertson, W., Schauer, J.J., Dwyer, H., Collins, J., Huai, T.,
558 Ayala, A., 2009. Metals emitted from heavy-duty diesel vehicles equipped with advanced PM and
559 NO_x emission controls. Atmospheric Environment, 43, 2950-2959.

Intergovernmental Panel on Climate Change (IPCC), 2007. Climate Change 2007: "The Physical Science Basis" Contribution of Working Group I to the Fourth Assessment Report of the Intergovernmental Panel on Climate Change. Cambridge University Press, New York.

Keegan, T.J., Faragó, M.E., Thornton, I., Hong, B., Colvile, R.N., Pesch, B., Jakubis, P., Nieuwenhuijsen, M.J., 2006. Dispersion of As and selected heavy metals around a coal-burning power station in central Slovakia. Science of the Total Environment, 358, 61-71.

Lim, H.J., Turpin., B.J., 2002. Origins of primary and secondary organic aerosols in Atlanta: Results of Time-resolved measurements during the Atlanta Supersite Experiment. Environmental Science and Technology, 36, 4489-4496.

Maenhaut, W., Raes, N., De Backer, H., Cheymol, A., 2007. Seasonal variability in atmospheric aerosol levels and elemental compositions during 2006 at Uccle, Belgium, In: Proceedings of the XI. International Conference on PIXE and its Analytical Applications, Puebla Mexico, May 25-29, 2007.

Maenhaut, W., 2008. New Direction: future needs for global monitoring and research of aerosol composition. Atmospheric Environment, 42, 1070-1072.

Manoli, E., Voutsa D., Samara, C., 2002. Chemical characterization and source identification/apportionment of fine and coarse air particles in Thessaloniki, Greece. Atmospheric Environment, 36, 949-961.

Matsumoto, K., Hayano, T., Uematsu, M., 2003. Positive artifact in the measurement of particulate carbonaceous substances using an ambient carbon particulate monitor, Atmospheric Environment, 37, 4713-4717.

Nriagu, J.O., Pacyna, J.M., 1988. Quantitative assessment of worldwide contamination of air, water and soils by tracemetals, Nature, 333, 134-139.

Oravisjärvi, K., Timonen, K.L., Wiikinkoski, T., Ruuskanen, A.R., Heinänen, K., Ruuskanen, J., 2003. Source contributions to $PM_{2.5}$ particles in the urban air of a town situated close to a steel works. Atmospheric Environment, 37, 1013-1022.

Pope, C.A., Dockery, D.W., 2006. Health Effects of Fine Particulate Air Pollution: Lines that Connect. Journal ofthe Air and Waste Management Association, 56, 709-742.

Putaud, J.P., Raes, F., Van Dingenen, R., Brüggemann, E., Facchini, M.C., Decesari, S., Fuzzi, S., Gehrig, R., Hüglin, C., Laj, P., Lorbeer, G., Maenhaut, W., Mihalopoulos, N., Müller, K., Querol, X., Rodriguez, S., Schneider, J., Spindler, G., ten Brink, H., Tørseth, K., Wiedensohler, A., 2004. A European aerosol phenomenology – 2: chemical characteristics of particulate matter at kerbside, urban, rural and background sites in Europe. Atmospheric Environment, 38, 2579-2595.

Querol, X., Alastuey, A., Ruiz, C.R., Artiñano, B., Hansson, H.C., Harrison, R.M., Buringh, E., ten Brink, H.M., Lutz, M., Bruckmann, P., Straehl, P., Schneider, J., 2004. Speciation and origin of PM10 and PM2.5 in selected European cities. Atmospheric Environment, 38, 6547-6555.

Pio, C.A., Nunes, T.V., Borrego, C.A., Martins, J., 1989. Assessment of air pollution sources in an industrial atmosphere using principal component/multilinear regression analysis. Science of the Total Environment, 80, 279-292.

Ravindra, K., Stranger, M., Van Grieken, R., 2008. Chemical characterization and multivariate analysis of atmospheric $PM_{2.5}$ particles. Journal of Atmospheric Chemistry, 59, 199-218.

Samek, L., Injuk, J., Van Espen, P., Van Grieken, R., 2002. Performance of a new compact EDXRF spectrometer for aerosol analysis. X-Ray Spectrometry, 31, 83-86.

ten Brink, H., Hoek, G., Khlystov, A., 2005. An approach to monitor the elemental carbon in the ultrafine aerosol. Atmospheric Environment, 39, 6255-6259.

Turpin, B.J., Huntzicker, J.J., 1991. Secondary formation of organic aerosol in the Los Angeles basin: a descriptive analysis of organic and elementary carbon concentrations. Atmospheric Environment, 25A, 207-215.

Turpin, B.J., Lim, H.J., 2001. Species contributions to PM2.5 mass concentrations: Revisiting common assumptions for estimating organic mass. Aerosol Science and Technology, 35, 602-610.

Twomey, S., 1974. Pollution and planetary albedo. Atmospheric Environment, 8, 1251-1256.

Vallius, M., Janssen, N.A.H., Heinrich, J., Hoek, G., Ruuskanen, J., Cyrys, J., Van Grieken, R., de Hartog, J.J., Kreyling, W.G., Pekkanen, J., 2005. Sources and elemental composition of ambient $PM_{2.5}$ in three European cities. Science of the Total Environment, 337, 147-162.

Vecchi, R., Valli, G., Fermo, P., D'Alessandro, A., Piazzalunga, A., Bernardoni, V., 2009. Organic and inorganic sampling artefacts assessment. Atmospheric Environment, 43, 1713-1720.

Vekemans, B., Janssens, K., Vincze, L., Adams, F., Van Espen, P., 1994. Analysis of X-ray spectra by iterative least squares (AXIL): new developments. X-Ray Spectrometry, 23, 278-285.

Viana, M., Maenhaut, W., Chi, X., Querol, X., Alstuey, A., 2007. Comparative chemical mass closure of fine and coarse aerosols at two sites in south and west Europe: Implications for EU air pollution policies, Atmospheric Environment, 41, 315-326.

Wang, Y.F., Huang, K.L., Li, C.T., Mi, H.H., Luo, J.H., Tsai, P.J., 2003. Emissions of fuel metals content from a diesel vehicle engine, Atmospheric Environment, 4637-4643.

Viana, M., Kuhlbusch, T.A.J., Querol, X., Alastuey, A., Harrison, R.M., Hopke, P.K., Winiwarter, W., Vallius, M., Szidat, S., Prévôt, A.S.H., Hueglin, C., Bloemen, H., Wåhlin, P., Vecchi, R., Miranda, A.I., Kasper-Giebl, A., Maenhaut, W., Hitzenberger, R., 2008. Source apportionment of particulate matter in Europe: A review of methods and results. Aerosol Science, 39, 827-849.

Table 1. Time schedule of the sampling campaigns and average daily meteorological data with their variations (expressed as standard deviation – SD)

Location – campaign	***Sampling period (day/month/year)***	***Season***	***Average precipitation (mm day^{-1})***	***Air temperature (^{o}C)***	***Air pressure (hPa)***	***Relative humidity (%)***	***Wind speed (m s^{-1})***	***Main wind direction****	***n***
Petroleumkaai-1	18/09/2001-29/10/2001	A	3.0±6.0	14.9±1.8	1014±7	72±5	3.9±1.4	SW	36
Petroleumkaai-2	19/12/2002-23/02/2003	W	3.5±5.9	4.5±4.6	1013±13	73±7	4.4±1.4	S-SW/NE	52
Borgerhout-1	06/11/2001-10/12/2001	A-W	2.7±4.7	6.9±3.2	1024±11	75±5	3.6±1.6	SW	32
Borgerhout-2	10/02/2003-07/04/2003	W-Sp	0.9±1.8	7.1±3.9	1024±8	59±10	3.4±1.3	E/E-NE/SE	45
Zelzate-1	11/12/2001-30/01/2002	W	1.8±3.5	3.2±3.6	1022±13	81±25	5.5±2.6	SW/W-SW	51
Zelzate-2	13/08/2002-26/09/2002	Su-A	1.0±2.4	17±3.0	1018±4	83±7	3.3±1.2	N/N-NE	40
Hasselt-1	01/02/2002-26/03/2002	W-Sp	3.2±4.3	8.2±3.0	1010±9	67±7	5.5±2.1	SW/W-SW	46
Hasselt-2	27/09/2002-04/11/2002	A	2.1±3.0	11.5±2.1	1013±9	70±6	4.0±1.9	SW/W	38
Mechelen-1	16/05/2002-26/06/2002	Sp-Su	2.1±5.1	17.1±2.6	1014±7	60±6	3.7±0.9	SW	30
Mechelen-2	05/11/2002-03/01/2003	A-W	2.6±4.0	6.2±4.2	1012±11	74±7	3.8±1.4	S/SE/E	38
Wingene-1	27/03/2002-15/05/2002	Sp	1.3±2.3	10.2±2.5	1016±9	73±10	4.1±1.8	SW/N/N-NE	41
Wingene-2	27/06/2002-12/08/2002	Su	2.2±5.0	17.2±2.6	1014±5	79±6	3.6±1.1	SW/W/NW	45

Abbreviations: A –autumn, W – winter, Sp – spring, Su – summer,
n – the number of daily data used for calculating average concentrations
* – the main wind directions were extracted from the windrose of each site/campaign

Table 2. Daily average $PM_{2.5}$-data (µg m^{-3}) from standard TEOM units

Location	**Campaign 1**			**Campaign 2**		
	Min	*Max*	*Mean ± SD*	*Min*	*Max*	*Mean ± SD*
Petroleumkaai	8.2	30.8	17 ± 6	8.3	31.9	16 ± 6
Borgerhout	6.2	34.9	20 ± 8	12.0	47.0	28 ± 11
Zelzate	6.2	53.1	21 ± 11	5.7	30.1	16 ± 7
Hasselt	6.8	34.4	13 ± 6	6.8	30.8	15 ± 6
Wingene	6.5	45.1	20 ± 10	6.5	27.2	13 ± 5
Mechelen	7.4	26.7	14 ± 5	9.9	44.5	21 ± 9
Mechelen	8.0	27.0	13 ± 4	8.0[a]	51.0[a]	22 ± 10[a]

[a] data from simultaneous sampling with a second TEOM unit operated at 40 °C

Table 3. Daily $PM_{2.5}$-data (µg m^{-3}) from Partisol sampling and gravimetry (Teflon filters)

Location	**Campaign 1**			**Campaign 2**		
	Min	*Max*	*Mean ± SD*	*Min*	*Max*	*Mean ± SD*
Petroleumkaai	7.9	59.5	20 ± 11	6.3	61.6	21 ± 12
Borgerhout	0.2	62.7	29 ± 15	13.8	99.7	45 ± 22
Zelzate	1.6	67.7	26 ± 16	5.9	43.8	16 ± 8
Hasselt	5.5	59.0	19 ± 13	4.4	38.5	16 ± 8
Wingene	7.0	63.9	28 ± 16	5.2	23.2	11 ± 4
Mechelen	7.1	21.3	12 ± 7	9.2	60.1	24 ± 13

Table 4. Average $PM_{2.5}$ concentrations for the monitoring period and extrapolated annual values

Location	***Number of days sampled***	***$PM_{2.5}$ average ($\mu g\ m^{-3}$)***	
		Monitored with Partisol	*Extrapolated yearly*
Petroleumkaai	89	21	23
Borgerhout	76	38	29
Zelzate	91	22	21
Hasselt	82	17	20
Wingene	94	20	18
Mechelen	71	19	19

Table 5. Percentage of $PM_{2.5}$ due to elemental fraction (%)

Location	**Campaign – 1**			**Campaign – 2**		
	Min	Max	Mean ± SD	Min	Max	Mean ± SD
Petroleumkaai	2.4	10.9	6.3 ± 2.5	1.1	11.5	2.7 ± 2.0
Borgerhout	1.1	7.5	2.9 ± 1.2	0.9	4.0	2.2 ± 0.7
Zelzate	0.7	24.1	5.8 ± 5.5	1.0	12.9	4.0 ± 2.5
Hasselt	0.2	5.1	2.1 ± 1.1	1.8	14.6	4.3 ± 3.2
Wingene	0.4	6.3	2.1 ± 1.4	0.8	4.1	2.1 ± 0.8
Mechelen	0.1	15.1	2.8 ± 2.6	1.1	13.5	3.8 ± 2.8

SD – standard deviation

Table 6. Average elemental concentrations in $PM_{2.5}$ over various sites and campaigns

Location – campaign	***Season***	***Average concentration (ng m^{-3})***													
		K	**Ca**	**Ti**	**V**	**Cr**	**Mn**	**Fe**	**Ni**	**Cu**	**Zn**	**Rb**	**Pb**	**Al**	**Si**	**Total**
Petroleumkaai-1	A	122	104	11	9	2	9	188	6	6	57	n.d.	13	122	366	1015
Petroleumkaai-2	W	139	3	5	16	1	4	66	7	4	31	1	26	83	58	444
Borgerhout-1	A-W	175	79	2	5	2	11	197	8	10	70	n.d.	28	55	186	828
Borgerhout-2	W-Sp	269	78	8	9	3	10	253	6	13	83	2	49	106	118	1007
Zelzate-1	W	247	111	6	6	1	13	279	9	7	84	1	24	60	302	1151
Zelzate-2	Su-A	104	63	6	8	1	3	95	4	5	20	1	15	51	181	557
Hasselt-1	W-Sp	93	32	2	n.d.	n.d.	4	56	3	3	33	n.d.	8	21	74	329
Hasselt-2	A	239	91	3	4	3	8	144	9	7	65	2	26	55	42	698
Mechelen-1	Sp-Su	69	34	1	1	2	5	60	4	5	31	1	8	29	74	324
Mechelen-2	A-W	183	91	3	3	3	9	127	8	9	66	2	30	46	35	615
Wingene-1	Sp	85	21	1	7	1	4	57	3	2	22	2	13	34	66	318
Wingene-2	Su	66	20	1	5	1	3	31	3	1	14	1	10	28	38	222
Overall average	**-**	**149**	**61**	**4**	**7**	**2**	**7**	**129**	**6**	**6**	**48**	**1.4**	**21**	**58**	**128**	**626**
SD	-	72	37	3	4	1	3	83	2	3	25	1	12	32	110	315

Abbreviations: A – autumn; W – winter; Sp – spring; Su – summer; n.d. – not detected

Table 7. Daily concentrations of EC and OC, and related OM and OC/EC ratios

Location – campaign	**Season**	**EC (µg m^{-3})**			**OC (µg m^{-3})**			**OC/EC**	**OM***	**OM+EC**
		Min	*Max*	Mean ± SD	*Min*	*Max*	Mean ± SD	*Mean*	*Mean*	*Mean*
Petroleumkaai – 1	A	0.2	3.3	1.1 ± 0.8	2.0	7.3	4.1 ± 1.3	3.7	6.6	7.7
Petroleumkaai – 2	W	0.1	1.1	0.4 ± 0.3	0.7	7.6	2.3 ± 1.3	5.8	3.7	4.1
Borgerhout – 1	A-W	0.1	4.4	1.3 ± 1.0	1.3	4.9	2.5 ± 1.1	1.9	4.0	5.3
Borgerhout – 2	Wi-Sp	0.5	3.1	1.5 ± 0.6	1.0	5.6	2.9 ± 1.3	1.9	4.6	6.1
Zelzate – 1	W	0.0	1.9	0.6 ± 0.5	1.1	5.9	2.6 ± 1.5	6.5	4.2	4.8
Hasselt – 2	A	0.1	1.1	0.3 ± 0.2	1.3	5.6	2.7 ± 1.1	9.0	4.3	4.6
Mechelen – 2	A-W	0.1	1.5	0.5 ± 0.3	2.0	10.2	4.2 ± 1.6	8.4	6.7	7.2

Abbreviations: A – autumn; W – winter; Sp – spring; SD – standard deviation;

* OM was calculated with a multiplication factor of 1.6

Table 8. Minimum and maximum concentrations of EC and OC measured by the ACPM (2-hour data)

Location – campaign	**EC (µg m^{-3})**		**OC (µg m^{-3})**	
	Min.	*Max.*	*Min.*	*Max.*
Petroleumkaai – 1	0.014	7.42	0.014	18.5
Petroleumkaai – 2	0.025	1.72	0.391	8.75
Borgerhout – 1	0.001	19.2	0.001	19.9
Borgerhout – 2	0.444	5.05	0.465	10.3
Zelzate – 1	0.001	9.22	0.001	12.3
Hasselt – 2	0.006	3.09	0.858	8.06
Mechelen – 2	0.061	1.91	1.15	13.5

Table 9. Percentage of the $PM_{2.5}$ concentration due to total carbon (EC+OC)

	Campaign – 1			**Campaign – 2**		
Location	*Min*	*Max*	Mean ± SD	*Min*	*Max*	Mean ± SD
Zelzate	3	77	14 ± 17	-	-	-
Hasselt	-	-	-	11	49	23 ± 8
Mechelen	-	-	-	7	71	24 ± 13
Petroleumkaai	9	48	32 ± 8	8	23	14 ± 4
Borgerhout	8	48	14 ± 8	4	22	12 ± 4

Fig. 1. Map of Flanders showing the six sampling sites

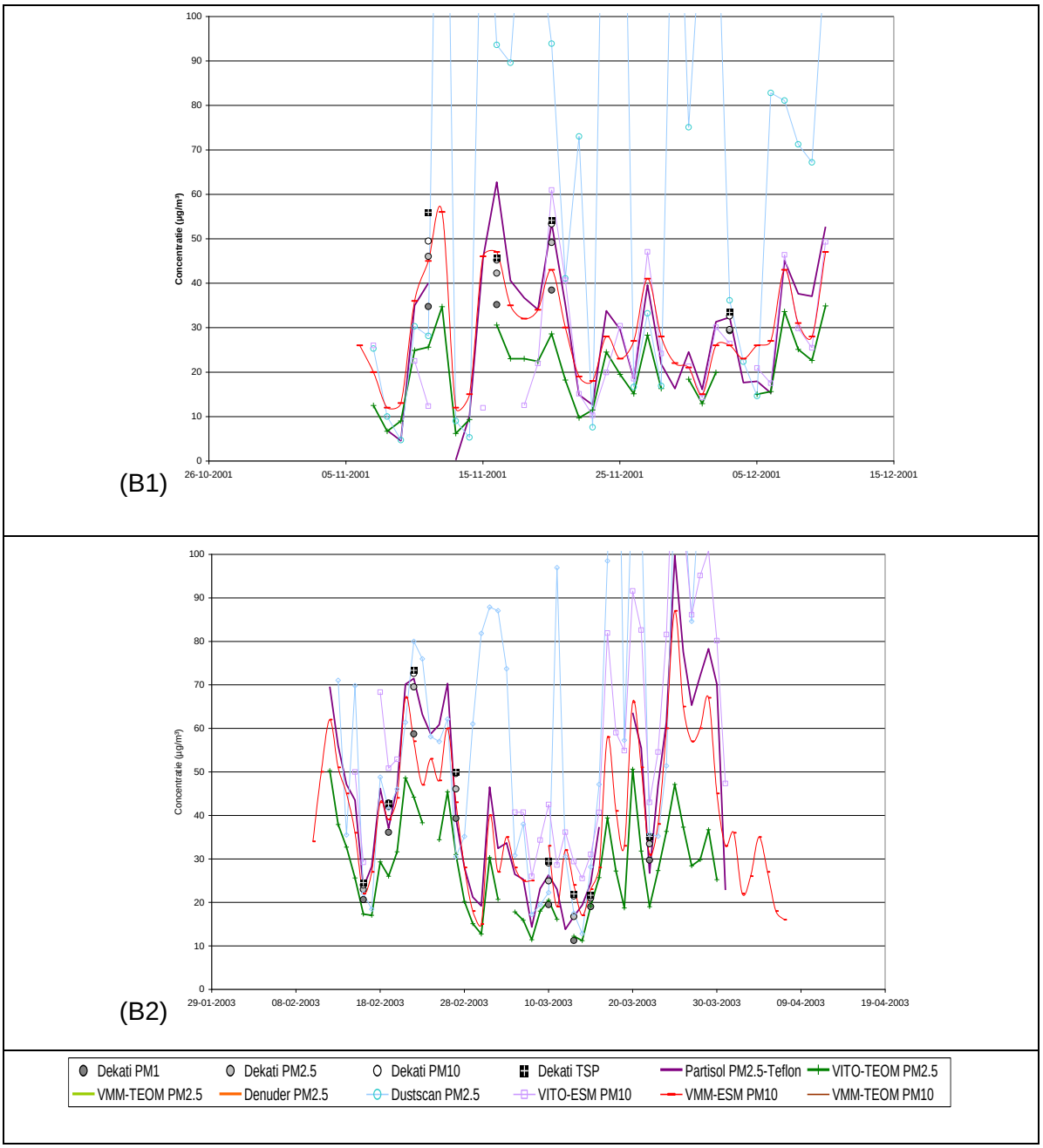

Fig. 2. Temporal variation of PM-concentrations in Borgerhout in campaign 1 (B1) and campaign 2 (B2) obtained with various methods

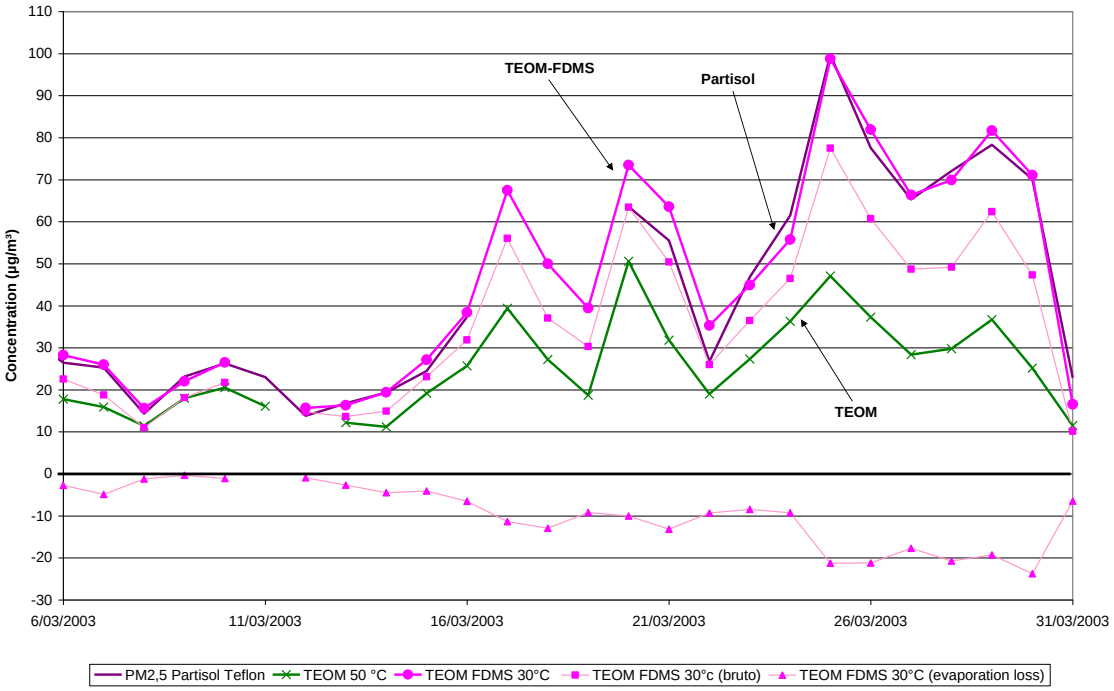

Fig. 3. Comparison of TEOM, TEOM-FDMS and Partisol sampling with gravimetry for the mass of $PM_{2.5}$ aerosols at Borgerhout in campaign 2 (bruto: the mass at 30 ^{o}C obtained after correction with the evaporation loss)

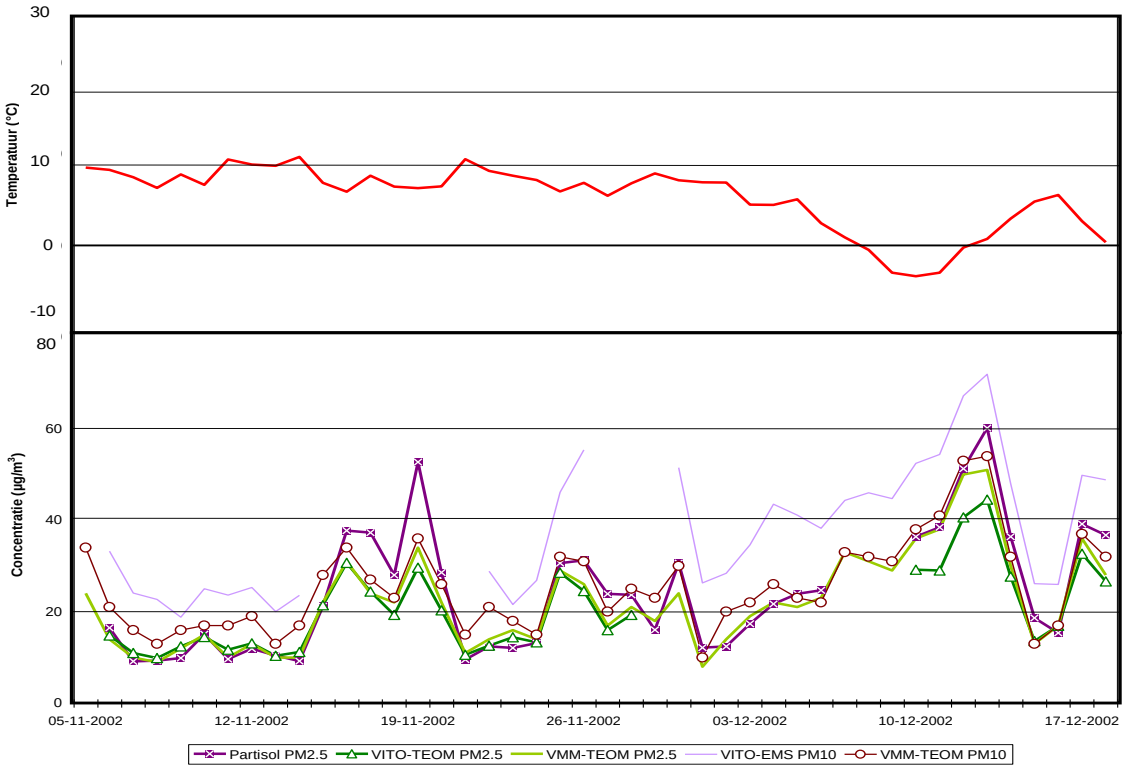

Fig. 4. Temporal fluctuation of the $PM_{2.5}$ and PM_{10} mass fractions and the average daily temperature in the second campaign in Mechelen

Supplementary Material

Supplementary Table 1
Correlation of PM elemental content, elemental and organic carbon, and meteorological parameters at various sampling sites and campaigns

	Z1	*Z2*	*B1*	*B2*	*P1*	*P2*	*H1*	*H2*	*M1*	*M2*	*W1*	*W2*
$PM_{2.5}$	**EC, OC, TC, RH(a), PR(a), T(a), WS(a), P_a**	**T_a**, **EC**	**EC,** PR(a), T(a), **WS(a), P_a**	**EC, OC, TC,** RH(a), PR(a), **T_a, P_a(a), WS(a)**	**EC, OC, TC, RH,** T_a(a), **WS(a)**	**EC, OC, TC, RH(a), PR(a), T_a(a), P_a**	**EC,** RH(a), **PR(a), T_a(a), P_a, WS(a)**	**EC, OC, TC,** RH, PR(a), T_a(a), **P_a, WS(a)**	PR, **T_a(a)**, P_a(a)	**EC,** RH(a), PR(a), **T_a(a)**, **P_a, WS(a)**	**RH(a), P_a, WS(a)**	**EC, T_a**, P_a
PM_{10}	**EC,** OC, **TC, RH(a), PR(a),** T_a(a), **WS(a), P_a**	T, RH, **EC**	-	**EC, OC, TC, RH(a),** PR(a), T_a, **WS(a)**	**EC,** TC, **RH**, T_a(a), P_a, **WS(a)**	**EC, OC, TC, RH(a), PR(a), T_a(a), P_a**	**EC, RH(a), PR(a), T_a(a), P_a, WS(a)**	**EC, OC, TC, T_a, P_a, WS(a)**	PR(a)	**EC, RH(a), PR(a), T_a(a), P_a,** WS(a)	-	**EC,** RH(a), **T_a**
K	Al, **Si, P, S**, **Cl,** Ca, **Mn**, **Ni, Cu, Zn, Br**, Sr, **Pb, EC,OC, TC**	**Al,** Si, **Ca**, V, **Mn, Fe**, Cu, **Zn, Rb**, **Pb,** T_a	**Al, Si, P, S, Cl, Ca**, V, **Mn, Fe, Cu, Zn, Br, Rb, Pb, EC, OC, TC, WS(a)**	**Al**, Cr, **Mn, Fe**, **Ni, Cu, Zn, Rb**, **Pb, EC, OC, TC,** RH(a), PR(a), WS(a)	Al, **Si, P, S, Ca, Mn, Fe**, **Ni, Cu, Zn,** Rb, **Pb, EC, OC, TC, WS(a)**	**Mn, Fe**, **Cu, Zn, Rb**, **Pb, EC, OC, TC,** PR(a), T_a(a), **P_a, WS(a)**	**Al, Si, P**, **S, Cl, Ca, Mn, Ni, Cu, Zn, Br, Pb**, **$PM_{2.5}$**	**Al**, **Ca, Mn, Ni, Cu, Rb, Sr, RH**	**Al, Si, Ca,** Ti(a), **Mn, Ni, Cu, Zn, Br**	Fe, Cu	Si, **Cr, Mn, Fe**, Ni, **Zn**, Rb, **Pb**, T_a(a)	**Al**, Fe, Cu, **Zn**, Pb, **EC**
Ca	**P**, S, Cl, **Ni, Cu**, RH	**Al, Si,** Ti, **Mn, Fe**, Cu**, Zn,** Rb**, Pb, EC**	**Al, Si, P,** S**, Cl,** V, **Mn, Fe, Ni**, **Cu, Zn,** Br, EC	**Al, Si, Ti, Cr, Mn, Fe**, **Ni**, Cu**, EC, T_a, WS(a)**	Si, P, S, **Mn, Fe**, **Ni, Cu, Zn,** Se**, Pb, EC, OC, TC,** $PM_{2.5}$, **WS(a)**	-	**Al, Si, P, S, Cl, Mn, Ni, Cu, Zn, Br, Pb**	**Al**, **Mn, Ni, Cu, Rb, Sr, RH**, **PR**	**Al, Si,** Cl, **Mn, Ni, Cu, Zn, Br**	Mn, **Ni**, **Cu**, Sr, **Pb(a)**, EC(a), **PR**, WS	Cr, RH	PR, T_a(a)
Ti	T_a	**Al**, Si, **Cr, Mn, Fe**, Zn, Pb, **EC**	P, V, Ni	**Al**, **Si**, V, Cr, **Mn, Fe, Ni, Cu, EC, T_a, WS(a)**	P, Al, Si, Se, $PM_{2.5}$	**V, Si**	$PM_{2.5}$, RH, P_a(a)	EC, PM_{10}, P_a	S(a), **Cl**, $PM_{2.5}$(a)	-	Cl(a), Ni, **Br**,	-

V	Al, **P**, S, **Br**	Al, **Si**, **Ni**, Rb, Sr, PM_{10}	**Al, Si, P**, **S,** Cl, **Mn**, Fe, **Ni, Br**, EC	**Al**, **Si,** Fe, **Ni, WS(a)**	Ni, $PM_{2.5}$(a), WS(a), P_a	-	-	-	$PM_{2.5}$	-	**P**, **S**, **Ni**, **Br**, Pb**,**	**Ni**, $PM_{2.5}$**,** WS
Cr	Al, Si, **Cl**, Mn, Sr, **RH(a)**, **EC**, TC	$PM_{2.5}$**,** WS(a)	Cl, Se	Al, Si, **Mn, Fe**, Cu, RH(a)	-	**RH(a),** WS(a)	-	Mn, T_a(a)	**Mn, Ni, Cu, Zn, Br,** $PM_{2.5}$(a)	**Mn**, Fe, Zn,	Si, **Mn**, Fe, **Zn**, Rb, Pb, PR	**Zn**, Pb, $PM_{2.5}$
Mn	**Al, Si, Cl**, **Fe**, **Zn**, **Br**, Rb, **Pb, EC, TC**	**Al**, **Si**, **Fe**, Cu, **Zn**, **Rb**, T_a	**Al, Si, P**, **S, Cl**, **Fe**, **Zn**, **Br**, Rb, **Pb, EC, OC, TC**	**Al**, **Si, Fe**, Ni, **Cu**, **Zn**, **Rb**, **Pb**, **EC, OC,** TC**,** RH(a), **WS(a)**	Si**, P, S,** Cl(a), **Fe**, Ni**, Cu, Zn, Se, Pb, EC, OC, TC, PM2.5, WS(a)**	**Fe**, **Cu**, **Zn**, **Rb**, **Pb**, **EC**, OC, **TC**, PR(a), **Pa, WS(a)**	**Al, Si, P, S, Cl, Ni, Cu**, **Zn**, **Br**, **Pb**, **PM2.5**	**Al**, Fe, **Ni**, **Cu**, **Zn**, **Rb**, **Pb**, **PM2.5**, EC	**Al**, **Si,** Fe, **Ni**, **Zn**,	**Fe, Ni, Cu, Zn**, PR	**Fe**, **Zn**, Br, **Rb**, **Pb**, T_a(a)	**Fe,** Ni, Cu, Zn, Pb, RH(a)
Fe	**Al,** Cl, Zn**, Rb, Pb, EC, OC, TC**, **WS**, **Ta**, PR, P_a(a)	**Al**, Si, **Zn, Rb, Pb,** EC	**Al, Si, P**, **S, Cl**, **Cu, Zn, Br, Pb, EC, OC, TC,** T_a(a), **Pa,** PR(a), **WS(a)**	**Al**, **Si, Ni, Cu, Zn,** Rb, Pb, **EC, OC,** TC**, RH(a), Ta, WS(a)**	Al, **Si**, **P, S**, Ni, **Cu, Zn,** Br, Rb, Sr, **Pb**, **EC, OC, TC, PM2.5, WS(a)**	**Cu, Zn, Rb**, Pb, **EC, OC, TC, PR(a), Pa, WS(a)**	**S, Pb, EC,** P_a, WS(a)	**Zn**, **Pb**, **EC, OC, TC, WS(a), Pa**	**Al, Si,** P, **S**, Sr, **Pb**, **RH, Ta(a)**	Si, **Zn, Pb**, **EC**	**Al, Si, P, S,** Cu, **Zn**, Br, Rb, **Pb**,	**Al**, **Si, Cu, Zn, Pb, EC**, RH(a), **Ta, WS(a)**
Ni	**Si**, **P**, **Cl**, **Cu, Zn, Br**, Sr, OC, T_a, **RH**, PR	Al, Si, **PM10**	Se, T_a	**Al**, Si, Cu, **EC, OC, TC,** T_a, **WS(a)**	P**, Cu,** EC**, PM2.5, WS(a)**	-	**Al, Si, P, S, Cl, Cu**, **Zn**, **Br**, **Sr**, **Pb**,	**Al, Cu**, **Rb**, RH**, PR**	Al, **Cu, Zn, Br, PR(a)**	**Cu**, Pb(a), EC(a), **RH, PR**, WS	**Al,** P**, S,** Cu, **Br, Pb,** $PM_{2.5}$	$PM_{2.5}$
Cu	**Si, P**, **Cl, Zn, Br,** EC, **OC**, TC, T_a, RH, PR	Zn, Rb, Pb	**Al, Si, P, S, Cl, Zn, Br, Pb, EC, OC, TC,** PR(a), P_a, WS(a) WD(a)	**Al**, Si, **Zn**, Rb, **Pb, EC,** OC**,** TC**, RH(a)**	**P, S, Zn,** Br, **Pb, EC, OC, TC, WS(a)**	**Zn**, **Rb**, **Pb, EC,** OC**, TC, PM2.5**, PR(a), WS(a)	**Al, Si, P, S, Cl, Zn**, **Br**, **Pb**, **PM2.5**	**Al, Rb**, **RH**	Al, **Zn, Br**, Rb(a)	Sr, RH	**Al, P**	**Al**, Si, **Zn, Pb, EC**, **Ta**
Zn	**Si, Cl**, **Br, Pb, EC**, **OC**, **TC**, T_a, RH,	**Al**, Si, **Rb, Pb, RH(a)**, T_a, EC	**Al, Si, S, P, Cl**, **Br, Rb, Pb, EC, OC,**	Al, **Rb, Pb**, **EC, OC, TC,** RH(a)	Si, **P, S,** Br, **Pb**, **EC, OC, TC, PM2.5,**	**Rb, Pb**, **EC, OC, TC, PR(a), Pa,**	**Al, Si, S, Cl, Br**, **Pb**, **P, PM2.5**	**Al, Pb**, **EC**	**Al, Br**	Si, EC	Si, Br, Rb, **Pb**, T_a(a)	**Pb**, EC, $PM_{2.5}$

	PR		**TC, P_a, WS(a)**		**WS(a)**	**WS(a)**						
Rb	**Se, Pb, EC, OC, TC,** PM_{10}	Si, **Pb**, $PM_{2.5}$	**Al, Si, P, S, Cl,** EC, **OC, TC**	**Pb**, EC, OC, TC, **WS(a)**	EC, OC, TC, **WS(a)**	**Pb**, **EC, OC, TC, RH, PR(a), P_a**	-	**Al, Si(a)**	Sr, $PM_{2.5}$, RH, PR	Al, EC(a)	S, **Pb**	-
Sr	**Al, Si**	-	-	-	Si	-	Al	**Al**	Al	-	-	P_a(a)
Pb	**Al, Cl**, EC, **OC**, TC	**Al**, **Si**, T_a, WS	**Al, Si, P, S, Cl, $PM_{2.5}$, PM_{10}, EC, OC, TC, T_a(a), P_a, WS(a)**	**EC,** OC**, TC**	Al, **Si**, **P**, **S**, **EC, OC, TC, $PM_{2.5}$, WS(a)**	Al, **EC, OC, TC**, **$PM_{2.5}$**, PR(a), WS(a)	**Al, Si, P, S, Cl, $PM_{2.5}$**	**EC, OC, TC, WS(a), P_a**	**Al, Si, P, S, RH, T_a(a),**	**EC, RH, WS**	Al, Si, **P**, **S,** T_a(a)	**EC,** $PM_{2.5}$, WS(a)
Al	**Si, P, S, EC**	**Si**, EC, T_a	**Si, P, S, Cl, EC, OC, TC, $PM_{2.5}$, PM_{10}**	**Si,** EC**, OC, TC, RH(a), T_a, WS(a)**	**Si**, **P**, **S**, OC, **$PM_{2.5}$**, **T_a**	**Si**	**Si, P, S, Cl, $PM_{2.5}$**	RH,	**Si, PM_{10}, RH, T_a(a)**	Si	**P**, S, $PM_{2.5}$,	Si, **EC, T_a,** WS(a)
Si	P, S, **Cl**	-	**P**, **S, Cl, EC, OC, TC**	**EC, T_a, WS(a)**	**P**, **S**, Cl(a), EC**, OC, TC, $PM_{2.5}$, T_a**	-	**P, S, Cl,** $PM_{2.5}$	**EC, PM_{10}, T_a, P_a**	P, **S**, **RH, T_a(a)**	-	RH(a), T_a(a)	**EC, RH(a), T_a**
Br	**Al, Si, P, S, Cl,** Rb, Pb, **EC, OC, TC**	n.a.	**Al, Si, P, S, Cl, Rb, Pb, EC, OC, TC,** RH, WS(a)	n.a.	**P**, **S, Pb,** EC	n.a.	**Al, Si, P, S, Cl,** Pb, **$PM_{2.5}$**	n.a.	$PM_{2.5}$(a)	n.a.	P, S, **Pb**,	n.a.
S	P, Se, EC, P_a, T(a), WS(a)	n.a.	**P, Cl, EC, OC, TC, WS(a)**	n.a.	**P**, **EC, OC, TC, RH, WS(a)**	n.a.	**P, Cl, $PM_{2.5}$**	n.a.	**P, RH, T_a(a), PR**	n.a.	P, $PM_{2.5}$	n.a.
Cl	**T_a, RH, PR, WS, P_a(a)**	n.a.	**P, EC, OC, TC, WS(a)**	n.a.	**OC(a),** TC(a), **T_a(a)**	n.a.	**P**, $PM_{2.5}$	n.a.	**T_a**	n.a.	$PM_{2.5}$(a), **RH**	n.a.
P	P_a, **WS(a)**, **EC**, OC	n.a.	**EC, OC, TC, WS(a),** RH	n.a.	**EC, OC, TC, WS(a)**	n.a.	$PM_{2.5}$,	n.a.	**RH, T_a(a)**	n.a.	**Se**, $PM_{2.5}$	n.a.

Abbreviations: EC – elemental carbon, OC – organic carbon, TC – total carbon, RH – relative humidity, PR – precipitation, WS – wind-speed, T_a – air-temperature, P_a – atmospheric pressure, (a) – anti correlation, n.a. – not analyzed; bold letter: correlation is significant at the 0.01 level (strong correlation), normal letter: correlation is significant at the 0.05 level (some correlation)

Supplementary Table 2: PCA of elements at Petroleumkaai

Rotated Component Matrix †						
Species	**Factor**					
	1	**2**	**3**	**4**	**5**	**6**
Al	-0.01	0.94	-0.17	0.05	0.21	0.01
Si	0.09	0.91	-0.18	0.13	0.18	-0.13
P	0.73	0.58	-0.11	0.26	-0.07	-0.04
S	0.79	0.47	0.08	0.26	-0.08	-0.14
Cl	-0.27	-0.15	0.37	-0.22	-0.58	-0.11
K	0.92	0.11	0.26	-0.07	0.02	-0.02
Ca	0.55	-0.43	0.06	-0.38	-0.07	0.56
Ti	0.16	0.21	0.14	0.85	-0.15	0.17
V	-0.31	-0.04	-0.13	0.70	0.43	-0.10
Cr	-0.09	0.00	-0.57	0.04	-0.02	-0.76
Mn	0.00	-0.07	0.10	0.23	-0.27	0.80
Fe	0.90	-0.19	-0.17	-0.15	0.03	0.14
Ni	-0.07	-0.06	0.95	0.03	-0.02	0.15
Cu	0.87	-0.13	-0.12	-0.17	0.31	0.23
Zn	0.96	-0.12	-0.06	0.11	-0.02	0.07
Se	-0.26	-0.28	-0.30	0.11	-0.69	0.18
Br	0.48	0.20	0.04	0.51	0.48	0.17
Rb	0.01	-0.40	0.81	0.07	0.02	0.16
Sr	-0.28	0.07	-0.02	0.03	0.67	-0.30
Pb	0.88	0.38	-0.03	0.10	-0.01	-0.01
Eigenvalue	***6.58***	***4.24***	***2.40***	***1.72***	***1.43***	***1.02***
% Variance Explained	***32.90***	***21.19***	***12.02***	***8.59***	***7.17***	***5.12***
Major Sources	***Refinery***	***Crustal***	***Brake wear +***	***Heavy oil burning***		

Extraction Method: Principal Component Analysis.
Rotation Method: Varimax with Kaiser Normalization.
†*Rotation converged in 14 iterations.*

Supplementary Table 3: PCA of elements at Borgerhout

Rotated Component Matrix †					
Species	**Factor**				
	1	**2**	**3**	**4**	**5**
Al	0.97	0.14	0.04	-0.09	0.13
Si	0.95	0.22	0.05	-0.01	0.15
P	0.96	0.20	-0.04	-0.08	-0.02
S	0.94	0.16	-0.09	-0.11	-0.06
Cl	0.70	0.47	0.10	-0.23	0.09
K	0.94	0.31	-0.01	0.02	0.00
Ca	0.66	0.60	0.05	0.16	0.26
Ti	-0.19	-0.33	0.14	0.88	-0.17
V	0.68	0.10	-0.11	0.54	-0.18
Cr	0.11	0.03	0.94	0.15	0.01
Mn	0.39	-0.29	-0.62	0.25	0.19
Fe	0.51	0.80	0.13	-0.07	-0.11
Ni	-0.46	0.26	-0.30	0.45	0.37
Cu	0.29	0.93	0.05	-0.16	0.03
Zn	0.74	0.58	-0.09	-0.07	-0.09
Se	0.10	-0.01	-0.12	-0.10	0.80
Br	0.86	0.20	0.07	-0.08	0.26
Sr	-0.13	0.63	-0.20	0.07	-0.65
Pb	0.49	0.71	0.29	-0.17	-0.13
Eigenvalue	***9.96***	***2.57***	***1.59***	***1.52***	***1.12***
% Variance Explained	***52.40***	***13.52***	***8.39***	***8.01***	***5.9***
Major Sources	***Vehicular***	***Non-exhaust***	***Non-ferrous industry***	***Heavy oil burning***	

† *Rotation converged in 11 iterations.*

Supplementary Table 4: PCA of elements at Zelzate

Rotated Component Matrix †					
Species	**Component**				
	1	**2**	**3**	**4**	**5**
Al	0.78	0.09	0.11	0.31	0.12
Si	0.66	-0.30	0.39	0.09	-0.08
P	0.70	0.64	-0.13	0.08	0.10
S	0.62	0.73	-0.03	0.01	0.12
Cl	0.88	0.02	0.16	-0.09	-0.34
K	0.89	0.00	0.23	-0.06	0.20
Ca	0.06	-0.06	-0.08	0.93	0.08
Ti	-0.22	-0.05	-0.03	-0.14	-0.77
V	0.07	0.34	0.79	-0.01	-0.16
Cr	-0.16	0.83	0.23	0.03	-0.15
Mn	0.38	-0.09	0.70	-0.18	0.34
Fe	0.77	0.21	0.20	0.47	0.12
Ni	0.45	0.39	0.43	0.26	0.10
Cu	0.67	0.14	-0.10	0.49	0.21
Zn	0.92	0.07	0.18	0.11	0.21
Br	0.79	0.42	0.30	0.08	0.08
Sr	-0.16	-0.37	-0.08	-0.50	0.49
Rb	0.22	0.49	0.36	0.02	0.40
Pb	0.88	0.20	0.02	0.04	0.24
Eigenvalue	***8.87***	***2.11***	***1.79***	***1.30***	***1.13***
% Variance Explained	***46.70***	***11.12***	***9.40***	***6.82***	***5.96***
Major Sources	***Coke-Oven***	***Combustion***	***Traffic (diesel)***	***Soil/road dust***	

† *Rotation converged in 15 iterations.*

Supplementary Table 5: PCA of elements at Hasselt

Rotated Component Matrix †					
Species	**Component**				
	1	**2**	**3**	**4**	**5**
Al	-0.07	-0.14	-0.11	0.15	-0.74
Si	0.99	-0.08	0.03	0.04	0.05
P	-0.09	-0.01	0.60	-0.23	-0.03
S	0.90	0.36	-0.09	0.04	0.03
Cl	1.00	-0.05	0.00	0.00	-0.01
K	0.99	0.02	0.01	0.07	-0.01
Ca	0.99	-0.09	0.04	0.01	-0.01
Ti	0.05	-0.53	-0.17	0.31	0.67
V	-0.10	-0.07	-0.06	-0.92	0.09
Cr	-0.07	0.80	-0.16	-0.06	0.37
Mn	-0.02	-0.45	-0.22	0.53	0.08
Fe	0.07	0.93	0.01	0.06	-0.16
Ni	0.99	-0.14	0.03	0.03	-0.01
Cu	0.99	-0.01	-0.01	0.04	-0.04
Zn	0.99	0.11	-0.03	0.06	-0.03
Br	1.00	-0.03	0.01	-0.01	0.03
Rb	0.38	0.03	0.78	0.25	-0.10
Sr	-0.24	-0.08	0.67	0.06	0.42
Pb	0.86	0.45	-0.09	0.08	0.06
Eigenvalue	***9.73***	***2.52***	***1.58***	***1.33***	***1.25***
% Variance Explained	***51.20***	***13.24***	***8.33***	***6.98***	***4.61***
Major Sources	***Vehicular***	***Road Dust***	***Biomass***	***Tyre wear / brake lining***	

† *Rotation converged in 8 iterations.*

Supplementary Table 6: PCA of elements at Wingene

Rotated Component Matrix †						
Species	**Component**					
	1	**2**	**3**	**4**	**5**	**6**
Al	0.39	-0.16	0.79	0.14	-0.06	-0.24
Si	0.47	-0.46	-0.11	-0.11	-0.06	-0.44
P	0.44	0.19	0.51	0.53	0.35	-0.02
S	0.47	0.33	0.25	0.56	0.47	-0.04
Cl	-0.22	-0.06	-0.03	0.89	0.00	-0.07
K	0.84	0.05	0.17	-0.20	-0.20	0.21
Ca	0.18	-0.15	0.19	0.03	0.20	0.81
Ti	0.17	0.04	-0.23	-0.13	-0.17	0.79
V	0.01	0.67	-0.10	0.56	-0.06	-0.19
Cr	-0.36	-0.22	0.08	0.08	-0.76	-0.01
Mn	0.05	-0.75	-0.07	0.07	0.01	-0.01
Fe	0.78	-0.22	0.38	0.05	0.11	-0.11
Ni	0.39	0.74	0.25	0.16	0.22	-0.02
Cu	0.06	0.13	0.78	-0.09	-0.06	0.26
Zn	0.84	-0.08	0.20	0.02	-0.03	0.16
Se	0.30	0.18	-0.02	0.54	-0.60	0.31
Br	0.19	0.43	0.67	-0.01	0.22	-0.13
Rb	0.67	0.35	-0.03	-0.13	0.12	0.16
Sr	-0.36	-0.05	0.11	0.25	0.65	0.15
Pb	0.88	0.22	0.15	0.23	0.06	0.09
Eigenvalue	***5.98***	***2.99***	***2.05***	***1.79***	***1.52***	***1.39***
% Variance Explained	***29.88***	***14.97***	***10.25***	***8.95***	***7.61***	***6.94***
Major Sources	***Biomass***	***Fuel oil***	***Crustal***	***Sea salt***		

† *Rotation converged in 10 iterations.*

Supplementary Table 7: PCA of elements at Mechelen

Rotated Component Matrix †					
Species	**Component**				
	1	**2**	**3**	**4**	**5**
Al	0.87	0.30	-0.09	-0.33	0.02
Si	0.50	0.84	-0.16	-0.09	0.07
P	-0.06	0.96	0.12	-0.14	-0.09
S	0.15	0.97	-0.12	0.09	0.09
Cl	0.69	0.19	0.22	-0.05	0.01
K	0.97	0.23	-0.03	0.02	-0.05
Ca	0.93	0.35	-0.02	0.02	-0.03
Ti	0.00	0.18	-0.25	-0.86	0.21
V	-0.14	0.24	0.11	-0.16	0.91
Cr	-0.23	-0.42	0.72	-0.13	0.49
Mn	-0.29	0.18	-0.59	0.63	-0.15
Fe	0.10	0.96	-0.18	-0.15	0.13
Ni	0.16	-0.13	0.91	0.18	-0.07
Cu	0.79	0.16	0.52	0.04	0.10
Zn	0.98	-0.09	-0.03	-0.01	-0.09
Se	0.83	-0.45	-0.21	0.13	0.00
Br	0.93	0.09	0.21	-0.01	-0.25
Rb	0.25	0.77	-0.13	0.44	0.25
Sr	-0.06	0.55	-0.13	0.62	0.49
Pb	0.15	0.97	-0.12	0.09	0.09
Eigenvalue	***8.09***	***5.35***	***2.35***	***1.88***	***1.11***
% Variance Explained	***40.44***	***26.75***	***11.77***	***9.39***	***5.57***
Major Sources	***Local Industry***	***Road Dust***	***Tyre wear / brake lining***		

† *Rotation converged in 8 iterations.*